**Indonesian Journal of Chemistry and Environment**
Vol. 6, No. 2, December 2023, pp. 95~110
e-ISSN: 2599-3186 

# Virtual Screening, Pharmacokinetic Prediction, Molecular Docking and Dynamics Approaches in the Search for Selective and Potent Natural Molecular Inhibitors of MAO-B for the Treatment of Neurodegenerative Diseases

**Suwardi[1], Agus Salim[2], Joanda Ario Yudha Mahendra[3], Daniel Bima Aji Wijayanto[4], Nurul Azqiya Rochiman[5], Sigit Khoirul Anam[6] and Nur Hikmah[7]**
[1-7]Department of Chemistry, Universitas Negeri Yogyakarta, Indonesia

**Article Info**

***Article history:***

Received Nov 12th, 2023
Revised Dec 6th, 2023
Accepted Dec 11th, 2023

***Corresponding Author:***

Suwardi
Department of Chemistry
Universitas Negeri Yogyakarta

Email: suwardi@uny.ac.id

**ABSTRACT**

This research aims to find natural product compounds that have the potential to act as MAO-B inhibitors that are useful in the treatment of neurodegenerative diseases, through the stages: a) Virtual Screening, b) Molecule Docking, c) Pharmacokinetic and toxicity prediction, and d) Simulation approach Molecular dynamics.

The research steps include the following steps: a) searching for molecules in the ZINC15 data base that are similar to the natural ligand molecule (safinamide) obtained from the protein data bank (PDB code: 2v5z) and the control ligand L-DOPA. A total of 481 molecules were downloaded from the data base and then molecular docking was carried out using the autodock program on the MAO-B target in the 2v5z receptor. After carrying out the docking analysis, 48 ligand molecules were selected which had a binding affinity (ΔG/kcal/mol) that was smaller than the ΔG of the natural ligand and the control ligand and nine (9) ligand molecules were taken to be tested: (i) ligand-ligand interactions MAO-B with discovery studio, (ii) Absorption, Distribution, Metabolism and Excretion properties with SwissADME and (iii) toxicity using PROTOX-II. Molecular dynamics simulations were carried out to determine the stability of ligands in proteins. Ligand complex [CC(C)c1ccc(NC(=O)Cn2cnc3c2c(=O)n(C)c(=O)n3C)cc1]-2v5z was chosen to simulate for 100 ps. The results of the molecular docking study showed that there were 9 molecules that had binding affinity values that were smaller than the binding affinity of the natural ligand and the control ligand. Ligand and residue interactions are dominated by hydrogen bonds, donor-donor and pi-pi stacked interactions. Based on SwissADME, the Blood Brain Barrier (BBB) permeant on ligand number 1, 2, 3, 5, 6, and 9 shows that it is orally active and cannot pass through the BBB and will not cause any side effects, whereas ligand number 4, 7, 8, 10, and 11 can cross the BBB and may cause side effects. Based on the results of toxicity prediction (PROTOX-II), it is known that there are four (4) ligands in class V, five (5) ligands in class IV and the rest in class II. Hepatotoxicity, carcinogenicity, and Phosphoprotein (Tumor Suppressor) p53 in eleven ligands are predicted to be inactive and have a small probability. The stimulated [CC(C)c1ccc(NC(=O)Cn2cnc3c2c(=O)n(C)c(=O)n3C)cc1]-2v5z complex apparently still shows ligand-protein fluctuations so that its conformation is still unstable.

***Keyword:*** screening virtual, molecular docking, molecular dynamics simulations

## 1. INTRODUCTION

Neurodegenerative and brain-related diseases are a major concern among aging populations worldwide (Boulaamane, et al, 2021). Neurodegenerative diseases such as Parkinson's and Alzheimer's diseases have a multifactorial nature characterized by progressive loss of neurons in the brain (Kovacs, 2014). Parkinson's disease (PD) is defined primarily by the progressive loss of dopaminergic neurons in the substantia nigra pars compacta (SNpc) of the midbrain (Relja, 2004). More than six million people worldwide are affected today with a prevalence of 150 in every 100,000 people increasing with age and affecting 1% of the population over 60 years (Jeppsson, et al, 2012). Current pharmaceutical treatments for PD include levodopa or levodopa plus dopa-decarboxylase inhibitors, dopamine agonists, and catechol-O-methyl transferase (COMT)/monoamine oxidase B (MAO-B) inhibitors (DiPisa, 2015). Recently, other non-dopaminergic drugs have shown promising efficacy for alleviating PD symptoms such as adenosine A2Areceptor (AA2AR) antagonists (Rohit & Tiratha, 2019).

Monoamine oxidase B (MAO-B) is an outer membrane-binding mitochondrial flavoenzyme that functions in the oxidative deamination of dopamine in the striatum. Inhibition of MAO-B in the brain can slow the depletion of dopamine stores and increase endogenous levels of dopamine, and exogenously produced dopamine is provided with levodopa. Furthermore, MAO-B inhibitors can also provide neuroprotective effects by reducing the production of potentially dangerous byproducts of dopamine metabolism in the brain (Azam, 2012).

Two isoforms of monoamine oxidase (MAO), 1MAO A and MAO B, exist in humans and are both 60-kDa mitochondrial outer membrane-bound flavoenzymes that share 70% sequence identity. These enzymes have distinct and overlapping specificities in the oxidative deamination of neurotransmitters and amines contained in food, the development of specific reversible inhibitors has been a long-sought goal. Expression of MAO B levels in nervous tissue increases 4-fold with age, resulting in increased levels of dopamine metabolism and production of higher levels of hydrogen peroxide, which is thought to play a role in the etiology of neurodegenerative diseases such as Parkinson's and Alzheimer's disease. Thus, it is important that the development of specific and reversible MAO B inhibitors may lead to clinically useful neuroprotective agents. The new crystal structure of human MAO B in complex with several pharmacologically important inhibitors has been solved to 1.6-Å resolution. The access channel from the protein surface to the active site of the enzyme consists of two cavities, the entry cavity and the active site cavity (Frantisek, 2005).

Monoamine Oxidase (MAO) (EC 1.4.3.4) belongs to a family of flavin adenine dinucleotide (FAD)-dependent enzymes expressed in the outer mitochondrial membrane of nerve cells. The MAO enzyme is responsible for the oxidative deamination of monoamine neurotransmitters such as dopamine, adrenaline, and noradrenaline in the central nervous system (CNS) (DiPisa, 2015; Lidia, et l, 2020). The MAO enzyme exists in two isoforms, MAO-A and MAO-B which have 70% sequence similarity but differ in tissue distribution, substrates, and inhibitor preferences (DiPisa, 2015). The development of the first MAO inhibitors was abandoned due to side effects related to tyramine metabolism, which caused a cardiovascular crisis (Yasin, et al, 2020). However, a new class of selective MAO-B inhibitors is efficient in treating PD symptoms. It was also shown that this new class of selective MAO-B inhibitors did not have tyramine-related side effects. In addition, selective MAO-B inhibitors can act as neuroprotective agents by limiting the release of free radical species and may thereby reduce disease progression ((DiPisa, 2015; Cheng, 2013). MAO-A preferentially metabolizes serotonin while MAO-B preferentially deaminates 2-phenylethylamine and benzylamine. Dopamine, norepinephrine, and epinephrine are substrates of both isoforms in most animal tissues (Kato, et al, 2021).

During aging, MAO-B expression increases in the brain and is connected to increased dopamine metabolism resulting in increased production of reactive oxygen species (ROS) such as hydrogen peroxide (H2O2) inducing oxidative damage and apoptotic signaling events (Zubair,

Maulana & Mukaddas, 2020). Previously approved MAO-B inhibitors are selegiline and rasagiline which irreversibly inhibit MAO-B with IC50 values of 6.8 and 14 nM, respectively (Monika, et, al, 2010). The latest approved MAO-B inhibitor is safinamide which reversibly inhibits MAO-B with an IC50 value of 450 nM (Azam, Madi & Ali, 2012). Istradefylline, a caffeine-based inhibitor approved in Japan in 2013 and also approved for medical use in the United States in 2019 acts as a dual inhibitor of MAO-B and AA2AR. However, istradefylline was found to be a weak inhibitor of MAO-B (IC50 =28μM) which prompted further research on new substitutions in the caffeine core.

The MAO-A crystal structure (PDB ID: 2Z5Y) has a monopartite substrate cavity with a volume of ~550 Å3 while the MAO-B crystal structure has a bipartite cavity structure with an entrance cavity of ~290 Å3 and a substrate cavity of ~ 400 Å3 [17]. ILE-199 and TYR-326 separate these two cavities in MAO-B that function as "gate" residues and structural determinants for substrate and inhibitor recognition by MAO-B (Monika, et, al, 2010).

Structural studies revealed that MAO-B (PDB ID: 2V5Z) is formed by two monomers consisting of globular domains anchored to the membrane via a C-terminal helix [20]. MAO-B active site residues that have similarities to the MAO-A active site are TYR-60, LEU-164, PHE-168, GLN-206, ILE-198, ILE-316, PHE-343, TYR-398, and TYR -435. Meanwhile, the amino acids specific for MAO-B are located in the hydrophobic pocket formed by LEU-171, CYS-172, ILE-199, and TYR-326 (Azam, Madi & Ali, 2012). There is a large body of literature supporting the use and efficacy of natural products (NPs) in PD such as flavonoids, xanthones, phenolic derivatives, alkaloids, and caffeine. This natural resource and its derivatives have been reported for their potential to selectively inhibit MAO-B and may offer a safer alternative compared to conventional drugs. Additionally, caffeine has been used in several studies as a scaffold for the design of dual MAO inhibitors/AA2AR antagonists. Pretorius et al. synthesized a series of C-8 substituted caffeine analogs and found that compounds containing a 4-phenylbutadiene moiety were the most potent candidates for MAO-B and AA2AR. On the other hand, Azam et al. exploring many caffeine derivatives from the literature containing many substitutions through molecular docking and structure-activity relationship studies, it was found that the placement of the hydrophobic group on C8 is critical for MAO-B inhibition and AA2AR antagonism, whereas substitutions occurring on C1 and C3 are optimal for AA2AR but does not harm MAO-B. Although research on caffeine has been ongoing for decades, its naturally occurring derivatives have not been investigated in detail (Azam, Madi & Ali, 2012).

NPs and NP-based compounds are an ideal choice for scientists and researchers due to the broadspectrum activity of NPs with minimal or no toxic effects on human health. Literature has shown that caffeine among other NPs is a potent compound that has neuroprotective properties. Considering the relationship between neurodegeneration and oxidative stress due to mitochondrial imbalance and accumulation of reactive oxygen species (ROS), MAO-B was, and is, considered a valid therapeutic target to slow the progression of Parkinson's disease.

The three-dimensional (3D) complex structure formed between the drug target and the drug candidate plays an important role in structure-based drug design (SBDD), where the drug candidate molecule is designed concerning the 3D structure of the drug target. Thus, computational prediction of protein-ligand complex structures, i.e., computational docking, plays an important role in SBDD. For computational docking, various procedures have been proposed that can predict the structure of protein-ligand complexes with high accuracy. To evaluate the docking software, docking poses that provide root mean square deviations (RMSDs) for the experimental structures less than or equal to 2.0 are considered as reasonable poses. When at least one reasonable pose is obtained from computational docking, the docking experiment is considered successful. The success rate of many docking programs has been reported to be higher than 70%. However, some well-programmed software has a success rate of more than 80% (Kovacs, 2014; Relja, 2004). Although a reasonable docking pose is preferably obtained as the highest-scoring pose of the ligand, evaluation methods for docking poses without experimental knowledge have not been sufficiently developed (Kato, 2021).

Generally, computational docking programs produce several candidate structures for protein-ligand complexes. For efficient in silico drug design trials, one or more candidates must be selected for the next step of drug design. In many cases, known experimental results, such as structure-activity studies, can be used for candidate pose selection. If useful experimental results are not available, pose selection is done from the evaluation of the score function. Although this scoring method likely provides appropriate scores for candidate docking poses, previous data suggests that approximately 50% of the highest-ranked poses can be considered plausible structures. For this reason, classical molecular dynamics (MD) simulations are sometimes used for docking pose selection (Kato, 2021).

In this study, a substructure search was performed on a natural product database to retrieve caffeine-containing natural products because they are known for their neuroprotective properties and their potential to act as AA2AR antagonists, a validated target for PD. Structure-based virtual screening was used to evaluate the affinity of selected natural compounds towards MAO-B and AA2AR. ADMET properties were evaluated using the silicon method. Finally, molecular dynamics simulations were performed to study the interactions and stability between the selected compounds and MAO-B over the simulation time.

## 2. RESEARCH METHOD

### 2.1 Materials and tools

Retrieval of all available natural compounds based on the similarity structure of safinamide and L-DOPA, using the ZINC15 databases. These compounds were downloaded in SDF format for further analysis. The software used is autodock4 and autodock vina, MGLTools 1.5.7, Pymol, swissadme, protox-II, and Desmond while the hardware consists of a computer with an Intel Core i3 processor, 6 GB RAM, 64-bit Windows operating system.

### 2.2 Molecular Docking

#### 2.2.1 Receptor preparation and grid determination

The crystal structure of MAO-B (PDB ID: 2V5Z, resolution=1.7 Å) in complex with safinamide was taken from the RCSB Protein Data Bank (https: http://www.rcsb.org/). Residues with missing atoms were corrected using the AutoDockTools 1.5.6. Water molecules were removed since they were not involved in ligand binding. Since MAO-B is expressed as a dimer, only one chain was kept together with the FAD cofactor for molecular modeling studies to reduce computational costs. Finally, polar hydrogens and Kollman charges were added. Grid boxes were placed near the FAD cofactor with a distance of 1 Å. The dimensions of the lattice were chosen large enough (40 × 40 × 40 Å in the x, y, and z directions, respectively) to fit all the residues that form both active site cavities in the protein. The grid squares are positioned so as to cover the entire binding site and allow larger molecules to dock properly: 52.114 ×156.171 × 28.035 Å for MAO-B at x, y, and z directions. Finally, the resulting coordinates for the grid boxes are saved in a text file.

#### 2.2.2 Ligand preparation

The Selected compounds were split into multiple files, with each file containing one ligand. 3D conformations were generated for all compounds, geometric optimization was performed using the Merck molecular force field (MMFF94) implemented in the Open Babel chemistry toolbox. The minimized ligands were then prepared for molecular docking studies using the package of AutoDockTools 1.5.6. Partial charges, atomic types, and polar hydrogens are added to all compounds and then converted to PDBQT format.

### 2.3 Molecular dynamics simulation

Molecular dynamics simulations were carried out with the Desmond program for the SAG, L-DOPA, and Ligand 9 (CC(C)c1ccc(NC(=O)Cn2cnc3c2c(=O)n(C)c(=O)n3C)cc1) with 2v5z receptors.

All complexes were individually solvated by placing a box filled with water with a size of 10 with a single point charge (SPC) water model with periodic boundary conditions (PBC). After optimization, the system is simulated in the NPT ensemble maintained at a temperature of 300 K and pressure using the Nose-Hoover thermostatic algorithm. The analysis of the ligand-receptor interaction was carried out using a simulation interaction diagram tool. The results of the analysis in the form of RMSD and RMSF ligand-protein against the reference.

## 3. RESULTS AND ANALYSIS

3.1 Ligand with the best conformation and binding affinity (ΔG)

A total of 48 ligands screened in the ZINC15 database with the best and selected conformations and their binding affinity values (ΔG/kcal mol$^{-1}$) are presented in Table 1. The ligand is selected based on the binding affinity values which is smaller than the binding affinity of the natural ligand and the control ligand. The natural ligand is a ligand taken from the 2v5z receptor, namely (S)-(+)-2-[4-(Fluorobenzyloxy-Benzylamino) Propionamide] or abbreviated as SAG, while the control ligand is levodopa (3,4-dihydroxy-L-phenylalanine).

**Table 1** Binding affinity values (kcal mol$^{-1}$) of ligands in the 2v5z receptor

| **ZINC ID, Native Dan Control Ligand** | **SMILES** | ΔG/ (kcal mol$^{-1}$) |
|---|---|---|
| **SAG (native ligand)** | O=C(/C=C/c1ccc(O)c(O)c1)C[C@@H](Cc1ccc(O)c(O)c1)C(=O) | **-10,0** |
| **Levodopa (3,4-dihidroksifenilalanin) (ligand control)** | C1=CC(=C(C=C1CC(C(=O)O)N)O)O | **-6,2** |
| ZINC000070454608 | O=C(/C=C/c1ccc(O)c(O)c1)C[C@@H](Cc1ccc(O)c(O)c1)C(=O)O | -10,2 |
| ZINC000000901160 | O=C(/C=C/c1ccc(O)c(O)c1)O[C@@H](Cc1ccc(O)c(O)c1)C(=O)O | -10,3 |
| ZINC000085994783 | N[C@H](Cc1ccc(O)c(-c2c(O)c(O)c3c(c2O)C(=O)c2c(cc(O)c(C(=O)O)c2C(=O)O)C3=O)c1)C(=O)O | -10,2 |
| ZINC000014813266 | C[C@@H](Cc1ccc(O)cc1)[C@H](C)Cc1ccc(O)c(O)c1 | -10,0 |
| ZINC000043060554 | O=C(/C=C/c1cc(O)c(O)cc1/C=C/c1ccc(O)c(O)c1)O[C@H](Cc1ccc(O)c(O)c1)C(=O)O | -10,2 |
| ZINC000006487282 | COc1ccc(C[C@@H](C)[C@@H](C)Cc2ccc(O)c(O)c2)cc1O | -10,0 |
| ZINC000033832765 | COC(=O)[C@H](Cc1ccc(O)c(O)c1)OC(=O)/C=C/c1ccc(O)c(O)c1 | -10,0 |
| ZINC000013377898 | O=C(CCc1ccc(O)c(O)c1)C[C@@H](O)CCc1ccc(O)c(O)c1 | -10,1 |
| ZINC000031169380 | C[C@@H](Cc1ccc(O)c(O)c1)[C@@H](C)Cc1ccc(O)c(OC(=O)c2ccc(O)cc2)c1 | -10,5 |

| ZINC ID, Native Dan Control Ligand | SMILES | ΔG/ (kcal mol$^{-1}$) |
|---|---|---|
| ZINC000031169384 | C[C@@H](Cc1ccc(O)c(OC(=O)c2ccc(O)cc2)c1)[C@H](C)Cc1ccc(O)c(O)c1 | -10,0 |
| ZINC000031169388 | C[C@@H](Cc1ccc(O)c(O)c1)[C@H](C)Cc1ccc(O)c(OC(=O)c2ccc(O)cc2)c1 | -10,0 |
| ZINC000031169392 | C[C@H](Cc1ccc(O)c(O)c1)[C@H](C)Cc1ccc(O)c(OC(=O)c2ccc(O)cc2)c1 | -10,5 |
| ZINC000070455139 | O=C(CCc1ccccc1)C[C@H](O)CCc1ccc(O)c(O)c1 | -10,1 |
| ZINC000085506858 | O=C(/C=C/c1cc(O)c(O)c2ccc(-c3ccc(O)c(O)c3)cc12)O[C@H](Cc1ccc(O)c(O)c1)C(=O)O | -10,5 |
| ZINC000015203323 | O=C(O[C@H](Cc1ccc(O)c(O)c1)C(=O)O)c1cc(-c2ccc(O)c(O)c2)c2cc(O)c(O)cc2c1 | -11,2 |
| ZINC000013377934 | O=C(/C=C/CCc1ccc(O)c(O)c1)CCc1ccc(O)c(O)c1 | -10,2 |
| ZINC000070457399 | O=C(/C=C/c1ccc2c(c1)O/C(=C\c1ccc(O)c(O)c1)C(=O)O2)O[C@H](Cc1ccc(O)c(O)c1)C(=O)O | -10,7 |
| ZINC000002508009 | N[C@@H](Cc1ccccc1)C(=O)Nc1ccc2ccccc2c1 | -11,6 |
| ZINC000013377927 | Oc1ccc(CCCC[C@@H](O)CCc2ccc(O)c(O)c2)cc1O | -10,1 |
| ZINC000085506834 | O=C(/C=C/c1cc(O)c(O)cc1/C=C/c1ccc(O)c(O)c1)O[C@H](Cc1cc(O)c(O)c(O)c1)C(=O)O | -10,4 |
| ZINC000085506765 | O=C(/C=C/c1cc(O)c(O)cc1/C=C/c1cc(O)c(O)cc1-c1cccc(O)c1)O[C@H](Cc1ccc(O)c(O)c1)C(=O)O | -11,0 |
| ZINC000040873155 | O=C(/C=C/c1ccc(O)c2c1C=Cc1cc(O)c(O)cc1O2)O[C@H](Cc1ccc(O)c(O)c1)C(=O)O | -11,2 |
| ZINC000013341088 | O=C(/C=C/CCc1ccc(O)cc1)CCc1ccc(O)c(O)c1 | -10,2 |
| ZINC000105258759 | COC(=O)[C@@H](Cc1ccc(O)c(O)c1)OC(=O)/C=C/c1ccc(O)c(O)c1/C=C/c1ccc(O)c(O)c1 | -10,2 |
| ZINC000000001083 | O=C(/C=C/c1ccc(O)c(O)c1)OCCc1ccccc1 | -10,0 |
| ZINC000085506767 | O=C(/C=C/c1cc(O)c(O)c2ccc(-c3cc(O)c(O)cc3-c3cccc(O)c3)cc12)O[C@H](Cc1ccc(O)c(O)c1)C(=O)O | -10,7 |
| ZINC000002111079 | Cc1oc2cc3oc(=O)c(CCC(=O)N[C@@H](Cc4ccc(O)c(O)c4)C(=O)O)c(C)c3cc2c1C | -10,3 |
| ZINC000002111081 | Cc1oc2cc3oc(=O)c(CCC(=O)N[C@H](Cc4ccc(O)c(O)c4)C(=O)O)c(C)c3cc2c1C | -10,2 |
| ZINC000038138562 | O=C(/C=C/c1ccc(O)c2c1[C@H](C(=O)O)[C@H](c1ccc(O)c(O)c1)O2)O[C@@H](Cc1ccc(O)c(O)c1)C(=O)O | -10,0 |
| ZINC000070454961 | O=C(/C=C/c1ccc(O)c2c1[C@H](C(=O)O)[C@@H](c1ccc(O)c(O)c1)O2)O[C@@H](Cc1ccc(O)c(O)c1)C(=O)O | -10,7 |
| ZINC000217660893 | COc1cccc2[nH]c(C(=O)NC[C@@H]3CCCN4CCCC[C@H]34)cc12 | -10,3 |
| ZINC000604405978 | (COc1cccc2[nH]c(C(=O)NCCc3cn(C)c4ccccc34)cc12) | -11,3 |

| **ZINC ID, Native Dan Control Ligand** | **SMILES** | ΔG/ (kcal $mol^{-1}$) |
|---|---|---|
| ZINC000524731786 | (COc1cccc2[nH]c(C(=O)N[C@H]3CCCc4c3[nH]c3ccccc43)cc12 | -11,7 |
| ZINC000000128554 | Cn1c(=O)c2c(ncn2Cc2ccc(C(C)(C)C)cc2)n(C)c1=O | -10,8 |
| ZINC000000001301 | CN(C)c1ccc(Cn2cnc3c2c(=O)n(C)c(=O)n3C)cc1 | -10,2 |
| ZINC000000898145 | CC(C)c1ccc(NC(=O)Cn2cnc3c2c(=O)n(C)c(=O)n3C)cc1 | -11,0 |
| ZINC000037868689 | Cn1c(=O)c2c(nc(OCc3ccccc3)n2C)n(C)c1=O | -10,2 |
| ZINC000045483982 | Cn1c(=O)c2c(nc(/C=C/C=C/c3ccccc3)n2C)n(C)c1=O | -11,2 |
| ZINC000045373200 | Cn1c(=O)c2c(nc(OCc3cccc(F)c3)n2C)n(C)c1=O | -10,6 |
| ZINC000000851804 | Cn1c(=O)c2c(ncn2CC(=O)Nc2nc3ccccc3s2)n(C)c1=O | -10,7 |
| ZINC000000851779 | CC[C@H](C)c1ccc(NC(=O)Cn2cnc3c2c(=O)n(C)c(=O)n3C)cc1 | -10,8 |
| ZINC000045498298 | Cn1c(=O)c2c(nc(/C=C/C=C/c3cccc(F)c3)n2C)n(C)c1=O | -12,4 |
| ZINC000045337362 | Cc1cccc(COc2nc3c(c(=O)n(C)c(=O)n3C)n2C)c1 | -10,7 |

The binding affinity (ΔG) price data presented in Table 1 was chosen to be smaller than the ΔG price for the native ligand-2v5z interaction. The ΔG values for native ligand-2v5z and control ligand-2v5z are -10.0 and -6.2 kcal/mol respectively, while the other ligands screened are less than -10.0 kcal/mol. Some interactions of selected ligands with receptors are shown in Figures 1- 5 below,

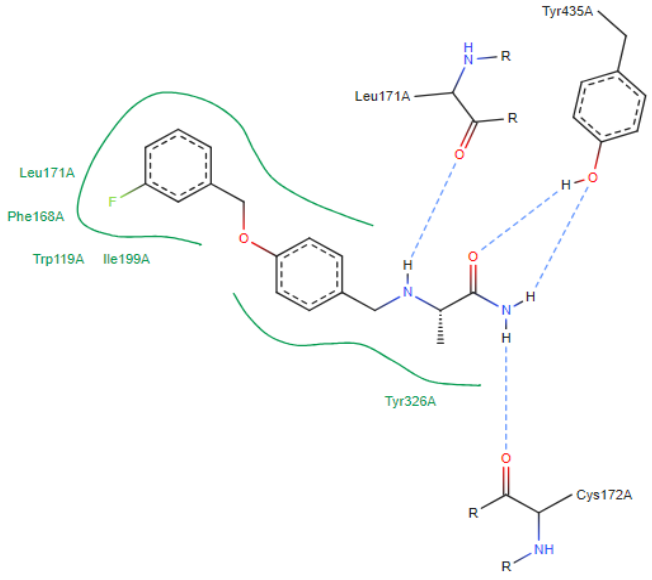


**Figure 1** The 2D interaction of SAG (safinamide) ligands with 2v5z receptors obtained from proteins.plus

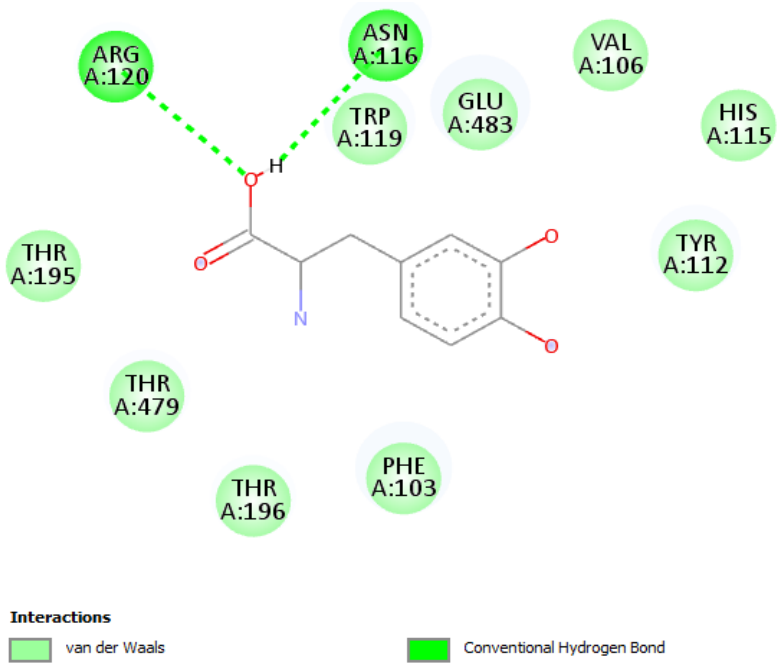


**Figure 2** The 2D interaction of 2v5z residue with control ligand levodopa (-6.2 kcal/mol) obtained via discovery studio visualizer

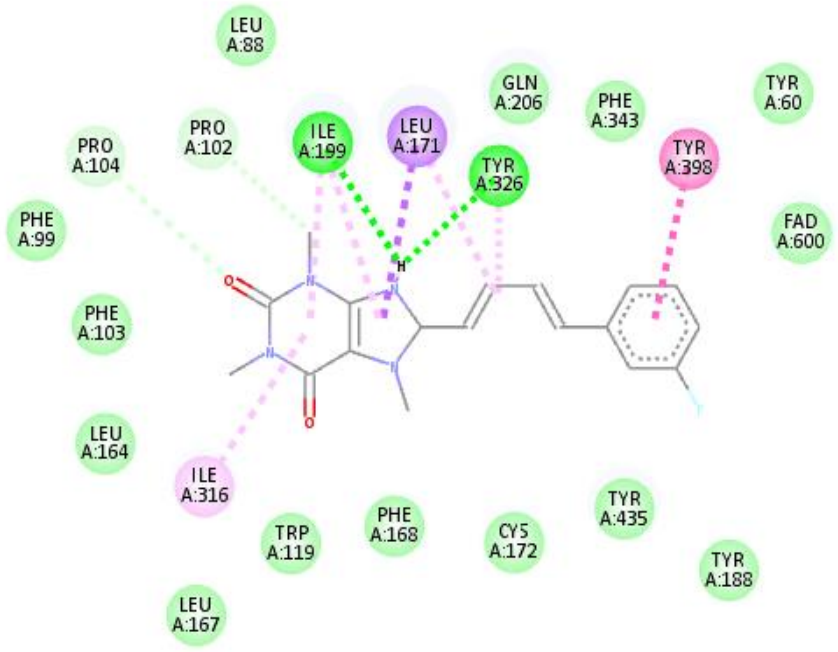


**Figure 3** The 2D interaction of residue 2v5z with ligand [Cn1c(=O)c2c(nc(_C=C_C=C_c3cccc(F)c3)n2C)n(C)c1=O] (-12.4 kcal/mol) obtained via discovery studio visualizer program

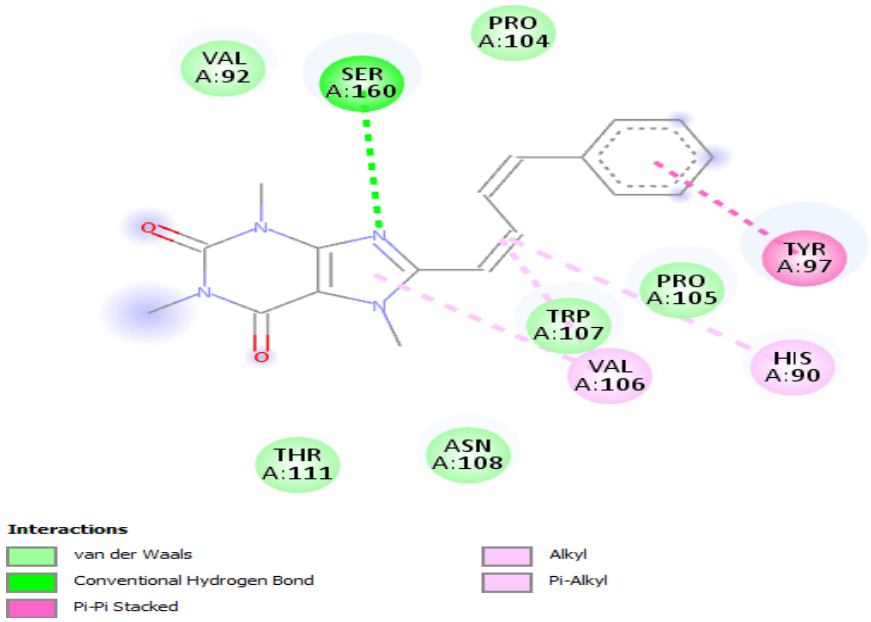


**Figure 4** The 2D interaction of residue 2v5z with ligand [Cn1c(=O)c2c(nc(_C=C_C=C_c3ccccc3)n2C)n(C)c1=O] (-11.2 kcal/mol) obtained via the discovery studio visualizer program

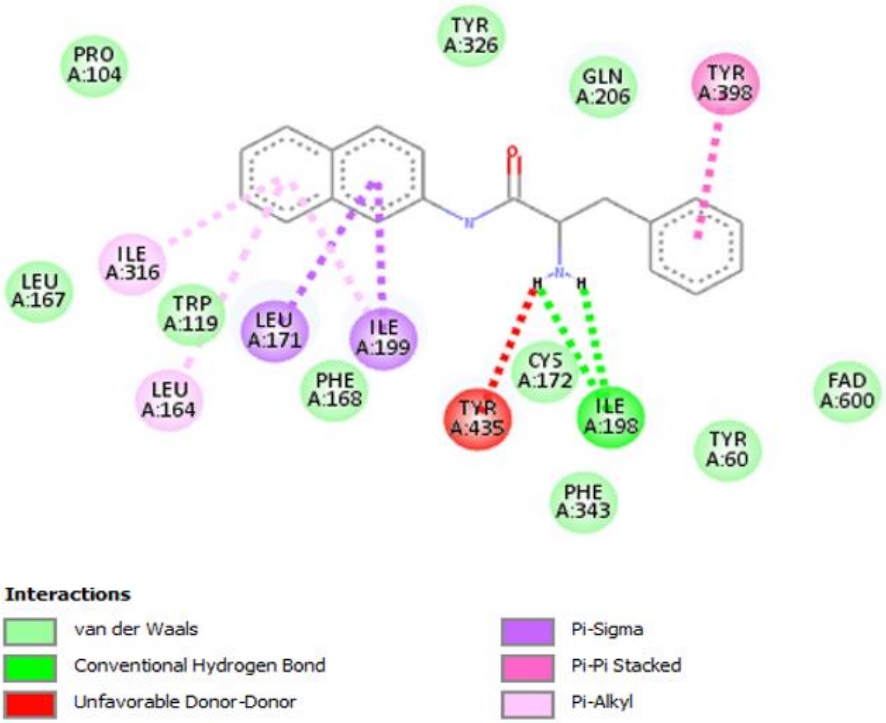


**Figure 5** The 2D interaction of residue 2v5z with ligand [N[C@@H](Cc1ccccc1)C(=O)Nc1ccc2ccccc2c1] (-11.6 kcal/mol) obtained through the discovery studio visualizer program

The interactions that can be observed in the figures are mainly hydrogen bond interactions, donor-donor interactions and stacked Pi-Pi. In general, the value of ΔG is related to the number of H-bond interactions. The more H-bonds, the lower the affinity binding value, so that it is better able to inhibit the target in the receptor, in this case monoamine oxidase B (MAO-B).

**3.2 Pharmacokinetic properties, and druglikes of ligands**

The pharmacokinetic, toxicity and druglike properties of nine (9) smiles structures with ΔG < -10.0 kcal/mol are presented in Table 2. ADMET prediction selection, namely absorption, distribution, metabolism, excretion and toxicity profiles, was carried out to determine drug candidates that are non-toxic and have a good oral pharmacokinetic profile, which is determined by the following parameters: high GI absorption, bioavailability score 0.55, grouped in class VI LD50 toxicity (more than 5,000 mg/kg), non-carcinogenic and non-mutagenic (Daina, Michielin, & Zoete, 2017; Martin, 2005). The pharmacokinetic properties (GI absorption, BBB permeant, bioavailability score, synthetic, Log S, Wlog P) and druglikes (Ro5) of the nine (9) screening ligands, native ligands and control ligands are presented in Table 3.

The SA (synthetic accessibility) value range is between 1 and 10, if the SA value is closer to 1, it means that the compound is easier to synthesize and conversely, the closer to 10 the compound is, the more difficult it is to synthesize (Ertl & Schuffenhauer, 2009). Eleven (11) selected compounds have SA values in the range 1< SA< 5, which indicates they are relatively easy to synthesize. Compounds can be classified according to solubility value (LogS). Compounds with solubility values of 0 and higher are highly soluble, compounds in the range 0 to −2 are soluble, compounds in the range −2 to −4 are slightly soluble, and insoluble if less than −4. In general, the selected ligand molecules have moderate solubility (slightly soluble). The property of lipophilicity shows that molecules can penetrate lipid membranes. Lipophilicity is characterized by the WLog P value. The Wlog P value of the ligand shown in table 3 is smaller than 5, which means the molecule can be explored as an important orally active molecule.

The bioavailability score has a score of around 0.55, meaning it does not become an anion at pH 6 and meets all Lipinski rules (Ro5), in this study there were 8 compounds that met this criterion, while three compounds had an NB of 0, 11 means that the compound will change to an anion (charge -1 or -2) at pH 6. The SWISS ADMET prediction, namely BBB (Blood Brain Barrier) is permeant to ligand compounds number 1, 2, 3, 5, 6, and 9, indicating that the orally active drug cannot pass through the BBB and will not cause any side effects, whereas ligand number 4, 7, 8, 10, and 11 can cross the BBB and may cause side effects.

**Table 2.** The Ligands (SMILES) are predicted by swissadme and protox-ii

| Number ligand | SMILES |
|---|---|
| 1 | O=C(/C=C/c1ccc(O)c(O)c1)C[C@@H](Cc1ccc(O)c(O)c1)C(=O)O as Native ligand Affinity binding (-10,0 kcal/mol) |
| 2 | C1=CC(=C(C=C1CC(C(=O)O)N)O)O [Levodopa (3,4-dihidroksifenilalanin)] as ligand control, Affinity binding (-6,2 kcal/mol) |
| 3 | O=C(O[C@H](Cc1ccc(O)c(O)c1)C(=O)O)c1cc(-c2ccc(O)c(O)c2)c2cc(O)c(O)cc2c1 Affinity binding (-11,2 kcal/mol) |
| 4 | N[C@@H](Cc1ccccc1)C(=O)Nc1ccc2ccccc2c1 Affinity binding (-11,6 kcal/mol) |
| 5 | O=C(/C=C/c1cc(O)c(O)cc1/C=C/c1cc(O)c(O)cc1-c1cccc(O)c1)O[C@H](Cc1ccc(O)c(O)c1)C(=O)O (-11,0 kcal/mol) |

| Number ligand | SMILES |
|---|---|
| 6 | O=C(/C=C/c1ccc(O)c2c1C=Cc1cc(O)c(O)cc1O2)O[C@H](Cc1ccc(O)c(O)c1)C(=O)O<br>Affinity binding (-11,2 kcal/mol) |
| 7 | (COc1cccc2[nH]c(C(=O)NCCc3cn(C)c4ccccc34)cc12)<br>Affinity binding (-11,3 kcal/mol) |
| 8 | (COc1cccc2[nH]c(C(=O)N[C@H]3CCCc4c3[nH]c3ccccc43)cc12<br>Affinity binding (-11,7 kcal/mol) |
| 9 | CC(C)c1ccc(NC(=O)Cn2cnc3c2c(=O)n(C)c(=O)n3C)cc1<br>Affinity binding (-11,0 kcal/mol) |
| 10 | Cn1c(=O)c2c(nc(/C=C/C=C/c3ccccc3)n2C)n(C)c1=O<br>Affinity binding (-11,2 kcal/mol) |
| 11 | Cn1c(=O)c2c(nc(/C=C/C=C/c3cccc(F)c3)n2C)n(C)c1=O<br>Affinity binding (-12,4 kcal/mol) |

**Table 3** Pharmacokinetic properties (GI absorption, BBB permeant, bioavailability score, synthetic accessibility, Log S, Wlog P) and druglikes (Ro5) of the nine (9) screening ligands, native ligands and control ligands

| Number ligand | GI absorption | BBB permeant | Lipinski rule of five (Ro5) | Bioavailability score | synthetic accessibility (SA) | solubility Log S | Lipophilicity (Wlog P) |
|---|---|---|---|---|---|---|---|
| 1 | high | no | yes | 0.56 | 3.33 | -3.22 | 2.32 |
| 2 | high | no | yes | 0.55 | 1.81 | 0.54 | 0.05 |
| 3 | low | no | yes | 0.11 | 3.75 | -5.47 | 3.59 |
| 4 | high | yes | yes | 0.55 | 2.22 | -4.01 | 3.16 |
| 5 | low | no | no | 0.11 | 4.69 | - 6.50 | 4.39 |
| 6 | low | no | yes | 0.11 | 4.54 | - 5.34 | 3.42 |
| 7 | high | yes | yes | 0.55 | 2.56 | -4.42 | 3.64 |
| 8 | high | yes | yes | 0.55 | 3.19 | -4.86 | 4.14 |
| 9 | tinggi | no | yes | 0.55 | 2.78 | -3.20 | 1.00 |
| 10 | high | yes | yes | 0.55 | 3.22 | -3.69 | 1.48 |
| 11 | high | yes | yes | 0.55 | 3.23 | -3.85 | 2.04 |

**3.3 Ligand Toxicity Properties**

Prediction of the toxicity of ligand molecules is carried out in a virtual laboratory (https://tox-new.charite.de/protox_II) and this is an important part in the search for new drugs or new drug design. Computational toxicity estimation is not only faster than determining toxic doses in animals, but can also help reduce the number of animal experiments. In this study, nine (9) ligand molecules obtained from the ZINC15 database, a native ligand and a control ligand (L-DOPA) were subjected to molecular docking tests (autodock Vina). The toxicity of the ligand molecule is then predicted based on the parameters hepatotoxicity, carcinogenicity, Phosphoprotein (Tumor Suppressor) p53 and $LD_{50}$. Toxicity and $LD_{50}$ of selected ligands are listed in Table 4.

The toxic dose is often given as the $LD_{50}$ value in mg/kg body weight. The $LD_{50}$ is the average lethal dose which means the dose at which 50% of test subjects die when exposed to a compound. Toxicity classes are determined based on the globally harmonized chemical labeling classification system (GHS). $LD_{50}$ values are given in [mg/kg]. The labeling classification of chemicals is stated in classes I to VI, namely class I: fatal if swallowed ($LD_{50} \leq 5$), class II: fatal if swallowed ($5 < LD_{50} \leq 50$), Class III: toxic if swallowed ($50 < LD_{50} \leq 300$), class IV: dangerous if swallowed ($300 < LD_{50} \leq 2000$), class V: possibly dangerous if swallowed ($2000 < LD_{50} \leq 5000$), and class VI: non-toxic ($LD_{50} > 5000$). Based on the data in Table 4.3, it is known that there are four (4) ligands in class V (ligand NO. 3-6), five (5) ligands in class IV (ligand NO. 1, 2, 7, 8 and 9) and the remaining entered class II (ligands No. 10 and 11). Hepatotoxicity, carcinogenicity, and Phosphoprotein (Tumor Suppressor) p53 in eleven ligands are predicted to be inactive and have a small probability. Therefore, the complex formed from ligands number 3, 4, 5, and 6 can be followed up for further research such as the stability of the ligand in the complex over a sufficient period of time through molecular dynamics simulations, in vitro and in vivo ligand tests.

**Table 4** Toxicity and $LD_{50}$ of selected ligands

| Number Ligand | Hepatotoxicity | Carcinogenecity | Phosphoprotein (Tumor Supressor) P53 | $Ld_{50}$ (Mg/Kg) |
|---|---|---|---|---|
| 1 | inactive probability =0.64 | inactive probability =0.59 | inactive probability =0.99 | 687 |
| 2 | inactive probability =0.58 | inactive probability =0.66 | inactive probability =0.75 | 1460 |
| 3 | inactive probability =0.65 | inactive probability =0.64 | inactive probability =0.81 | 4300 |
| 4 | inactive probability =0.66 | inactive probability =0.69 | inactive probability =0.83 | 3000 |
| 5 | inactive probability =0.60 | inactive probability =0.64 | inactive probability =0.73 | 5000 |
| 6 | inactive probability =0.70 | inactive probability =0.67 | inactive probability =0.71 | 5000 |
| 7 | inactive | inactive | inactive probability =0.83 | 650 |

| Number Ligand | Hepatotoxicity | Carcinogenecity | Phosphoprotein (Tumor Supressor) P53 | $Ld_{50}$ (Mg/Kg) |
|---|---|---|---|---|
| | probability =0.84 | probability =0.69 | | |
| 8 | inactive probability =0.71 | inactive probability =0.64 | inactive probability =0.83 | 500 |
| 9 | inactive probability =0.77 | inactive probability =0.69 | inactive probability =0.88 | 598 |
| 10 | inactive probability =0.89 | inactive probability =0.88 | inactive probability =0.94 | 19 |
| 11 | inactive probability =0.73 | inactive probability =0.83 | inactive probability =0.92 | 61 |

**4.3 Conformational stability of the ligand (9)-2v5z complex**

The stability of the ligand (9)-2v5z complex resulting from molecular dynamics simulations is indicated by fluctuations in the protein-ligand RMSD graph shown in Figure 6.

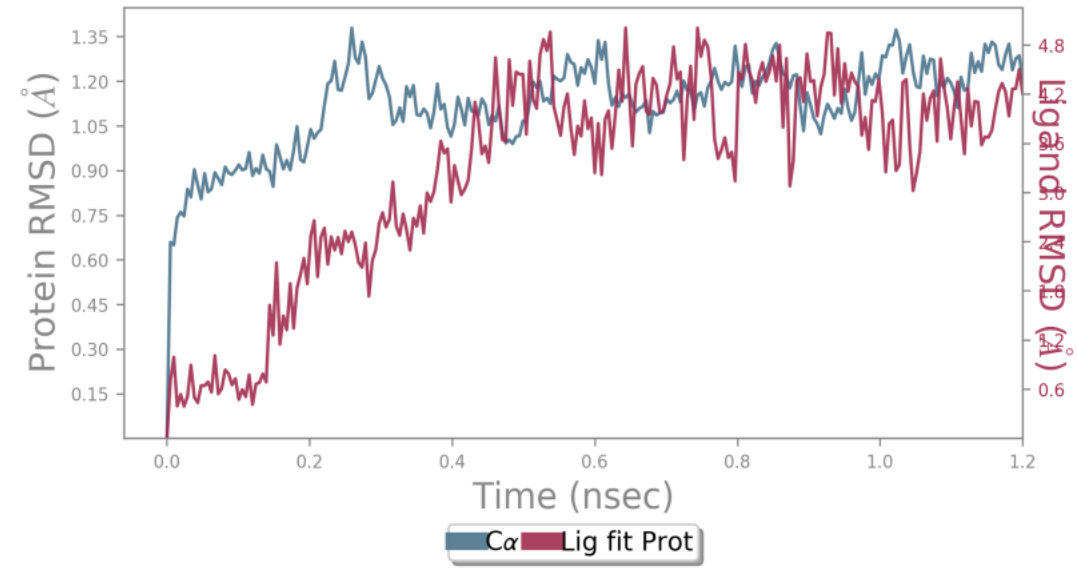


**Figure 6** Fluctuations of the ligand (9)-2v5z complex

The plot above shows the RMSD evolution of a protein (left Y-axis). All protein backbones are first aligned on the reference frame backbone, then RMSD is calculated based on the atom selection. Monitoring a protein's RMSD can provide insight into its structural conformation across parts of the simulation. RMSD analysis can show whether the simulation has reached equilibrium — its fluctuations towards the end of the simulation are around some thermal mean structure. Changes of the order of 1–3 Å are perfectly acceptable for small globular proteins. However, changes much larger than that indicate that the protein did undergo large conformational changes during the simulation. It is also important that the simulation converges — the RMSD value stabilizes around

a fixed value. If the protein RMSD is still increasing or decreasing on average at the end of the simulation, then your system has not reached equilibrium, and the simulation system may not be long enough for a thorough analysis. Ligand RMSD (right Y-axis) shows how stable the ligand is to the protein and its binding pocket. In the plot above, 'Lig fit Prot' shows the RMSD of a ligand when the protein-ligand complex is first aligned on a reference protein backbone and then the RMSD of the heavy atoms of the ligand is measured. If the observed value is significantly greater than the RMSD of the protein, it is likely that the ligand has diffused away from its initial binding site.

The Ligand-protein interactions can also be observed in Figure 7,

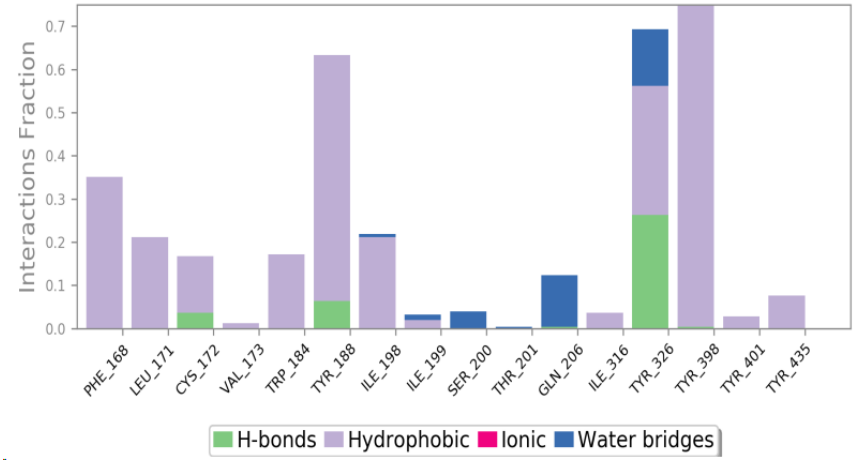


**Figure 7** The Ligand-protein interactions

Protein interactions with ligands can be monitored throughout the simulation. These interactions may occur categorized by type and summarized, as shown in the plot above. Protein-ligand interactions (or 'contacts') are categorized into four types: Hydrogen Bonding, Hydrophobic, Ionic and Water Bridges. Each interaction type contains more specific subtypes, which can be explored via the 'Simulation Interaction Diagram' panel. The stacked bar charts are normalized along the trajectory: for example, a value of 0.7 indicates that 70% of the simulation time a specific interaction is maintained. Values over 1.0 are possible because some protein residues can make multiple contacts of the same subtype with the ligand. Hydrogen Bonds: (H Bonds) play an important role in ligand binding. Consideration of hydrogen bonding properties in drug design is important because of its strong influence on drug specificity, metabolism and adsorption. Hydrogen bonds between proteins and ligands can be further broken down into four subtypes: backbone acceptor; contributing spine; side chain acceptor; side chain donor. Current geometric criteria for protein–ligand H bonds are: 2.5 Å distance between donor and acceptor atoms (D—H···A); donor angle ≥120° between donor-hydrogen-acceptor atoms (D—H···A); and an acceptor angle of ≥90° between the atoms bound to the hydrogen acceptor (H···A—X). Hydrophobic contacts: divided into three subtypes: π-Cation; π-π; and other non-specific interactions. Generally this type of interaction involves a hydrophobic amino acid and an aromatic or aliphatic group on the ligand, but we have expanded this category to also include π-Cation interactions. The current geometric criteria for hydrophobic interactions are as follows: π-Cation — Aromatic groups and charged groups within 4.5Å; π-π — Two aromatic groups arranged opposite or opposite each other; Other — Non-specific hydrophobic side chains within 3.6 Å of the aromatic or aliphatic carbon of the ligand. Ionic interactions: or polar interactions, occur between two oppositely charged atoms that are within 3.7 Å of each other and do not involve hydrogen bonds. We also monitor Protein-Metal-Ligand interactions, which are determined by metal ion coordination within 3.4 Å of protein and ligand heavy atoms (except carbon). All ionic interactions are broken down into two subtypes: those mediated by the protein backbone or side chains. Water Bridge is a hydrogen bonded protein-ligand

interaction mediated by water molecules. Hydrogen bond geometry is slightly looser than the standard H-bond definition. The current geometric criteria for protein–water H bonds or water ligands are: a distance of 2.8 Å between the donor and acceptor atoms (D—H···A); donor angle ≥110° between donor-hydrogen-acceptor atoms (D—H···A); and an acceptor angle ≥90° between the hydrogen-bonded acceptor atoms (H···A—X)

## 4. CONCLUSION

The conclusions that can be drawn from the molecular docking studies resulting from ZINC15 database screening and Swissadme and Protox-II predictions as well as DM simulations are:

a. There are 9 molecules that have a binding affinity value that is smaller than the binding affinity of the natural ligand and the control ligand. Ligand and residue interactions are dominated by hydrogen bonds, donor-donor and pi-pi stacked interactions.
b. According to Swissadme's predictions, the ligands that are predicted to be orally active and cannot pass through the BBB and will not cause side effects are ligands number 1, 2, 3, 5, 6, and 9 while ligand numbers 4, 7, 8, 10, and 11 can cross the BBB and may cause side effects.
c. Based on the results of toxicity prediction (PROTOX-II), it is known that there are four (4) ligands in class V, five (5) ligands in class IV and the rest in class II. Hepatotoxicity, carcinogenicity, and Phosphoprotein (Tumor Suppressor) p53 in eleven ligands are predicted to be inactive and have a small probability.
d. Ligand-protein fluctuations in the complex originating from the ligand [CC(C)c1ccc(NC(=O)Cn2cnc3c2c(=O)n(C)c(=O)n3C)cc1]-2v5z is still high, which indicates that the conformation is not yet stable.

**ACKNOWLEDGEMENTS**

This work was funded by RG grants (B/55/UN34.13/HK.03/2023) from Universitas Negeri Yogyakarta, Indonesia.

**REFERENCES**

Azam, F., Madi, A. M. & Ali, H.I. (2012). Molecular Docking and Prediction of Pharmacokinetic Properties of Dual Mechanism Drugs that Block MAO-B and Adenosine A2A Receptors for the Treatment of Parkinson's Disease. *Journal of Young Pharmacists* Vol 4 No 3, 184-192. https://doi.org/10.4103%2F0975-1483.100027

Boulaamane, Y., Ibrahim, M.A.A., Britel, M.R., and Maurady, A.,(2021). *In silico* studies of natural product-like caffeine derivatives as potential MAO-B inhibitors /AA2AR antagonists for the treatment of Parkinson's disease. *Journal of Integrative Bioinformatics*. 19(4), 0027. https://doi.org/10.1515/jib-2021-0027

Cheng, F., Li, W., Liu., and Tang, Y. (2013). In Silico ADMET Prediction: Recent Advances, Current Challenges and Future Trends. *Current Topics in Medicinal Chemistry*, 13, 1273-1289. http://dx.doi.org/10.2174/15680266113139990033

DiPisa, F.,. et.al. (2015). The soluble Y115E–Y117E variant of human glutaminyl cyclase is a valid target for X-ray and NMR screening of inhibitors against Alzheimer disease. *Acta Cryst*. ***71***, 986–992**.** https://doi.org/10.1107/S2053230X15010389

Jeppsson, F., *et. al*., (2012). Discovery of AZD3839, a Potent and Selective BACE1 Inhibitor Clinical Candidate for the Treatment of Alzheimer

Disease. *The Journal of Biological Chemistry*. 49, 287, 41245–41257. https://doi.org/10.1074/jbc.M112.409110

Kato, K., Nakayoshi, T., Kurimoto, E. & Oda, A. (2021). *Molecular dynamics simulations for the protein–ligand complex structures obtained by computational docking studies using implicit or explicit solvents. Chemical Physics Letters*. 781, 139022 . https://doi.org/10.1016/j.cplett.2021.139022

Kovacs, G.G. (2014). Current Concepts of Neurodegenerative Diseases. *Emj Neurol*, 1, 78-86. https://doi.org/10.33590/emjneurol/10314777

Lidia, C. et. al. (2020). Monoaryl derivatives as Transthyretin fibril formation inhibitors: design, synthesis, biological evaluation and structural analysis. *Bioorganic & Medicinal Chemistry*, ***115673***. https://doi.org/10.1016/j.bmc.2020.115673

Monika, G., Punam, G., Sarbjot, S., and Gupta G. D. (2010). An Overview on Molecular Docking. *Int.J. Drug Dev. & Res.*, 2(2):219-231. https://www.jscimedcentral.com/public/assets/articles/chemistry-4-1024.pdf

Relja, M. (2004). Pathophysiology and Classification of Neurodegenerative Diseases. *The Journal of The International Federation of Clinical Chemistry and Laboratory Medicine*, 15, 3, 097-099. https://www.ncbi.nlm.nih.gov/pmc/articles/PMC6034184/pdf/ejifcc-15-097.pdf

Shukla, R. & Singh, T. R. (2019). Virtual Screening, Pharmacokinetics, Molecular dynamics and binding free energy analysis forsmall natural molecules against Cyclin-dependent kinase 5 for Alzheimer's disease. Journal of Biomolecular Structure and Dynamics, 1538-0254. https://doi.org/10.1080/07391102.2019.1571947

Yasin, S.A. Azzahra, A. Ramadhan, N.E., dan Mylanda, V., (2020). Studi Penambatan Molekuler Dan Prediksi Admet Senyawa Bioaktif beberapa Jamu Indonesia Terhadap SARS-COV-2 Main Protease ($M^{pro}$). *BIMFI*, 2, 7 24-41.http://doi.org/10.48177/bimfi.v7i2.45

Zubair, M. S., Maulana, S. & Mukaddas, A. (2020). Molecular Docking and Molecular Dynamics Simulation of Compounds from Nigella Genus on Protease HIV-1 Enzyme Inhibitors. *Galenica Journal of Pharmacy*, 6(1), 132-140. https://dx.doi.org/10.22487/j24428744.2020.v6.i1.14982